

Mössbauer study of the vibrational anisotropy and of the light-induced population of metastable states in single-crystalline guanidinium nitroprusside

V. Rusanov¹, H. Winkler², C. Ober², and A.X. Trautwein^{2,a}

¹ Sofia University, Faculty of Physics, Department of Atomic Physics, 5 James Bouchier Blvd., 1126 Sofia, Bulgaria

² Medizinische Universität zu Lübeck, Ratzeburger Allee 160, 23538 Lübeck, Germany

Received 15 December 1998 and Received in final form 3 March 1999

Abstract. Mössbauer studies were performed on single crystals of guanidinium nitroprusside with different orientations of their principal crystallographic axes (**a**, **b**, **c**) with respect to the incident radiation. The markedly anisotropic Lamb-Mössbauer factor f_{LM} , *i.e.* $f_{LM}^{(a)} = 0.118(8)$, $f_{LM}^{(b)} = 0.174(8)$, $f_{LM}^{(c)} = 0.202(8)$ is in contrast to that of nitroprussides with inorganic anions. The observed anisotropy is ascribed to the anisotropic vibrational mean-square displacement of the nitroprusside anions as a whole which is due to the specific packing of both, anions and cations, as well as the very weak chemical bonding between the ions, typical only for guanidinium nitroprusside. The vibrational anisotropy of iron atoms in barium nitroprusside that has been observed by X-ray structural investigations has a different origin and therefore does not result in an anisotropic Lamb-Mössbauer factor. We have also investigated metastable states in guanidinium nitroprusside that have been populated by means of incoherent irradiation from light-emitting diodes. With a specific orientation of the guanidinium nitroprusside single crystal a population of the metastable states up to 26% could be achieved. Populations of comparable size on lithium, sodium and potassium nitroprussides have only been reached using coherent laser irradiation.

PACS. 63.20.Dj Phonon states and bands, normal modes, and phonon dispersion – 76.80.+y Mössbauer effect; other γ -ray spectroscopy – 39.30.+w Spectroscopic techniques

1 Introduction

Previous measurements on powder samples [1] of nitroprussides with inorganic cations, *e.g.* Na^+ , K^+ , Ca^{++} , or Ba^{++} , exhibit Mössbauer absorption spectra with a quadrupole doublet of equal line intensities. However, nitroprussides with organic cations, including the guanidinium ion $(\text{CN}_3\text{H}_6)^+$, show a pronounced asymmetry in the intensities of the two quadrupole lines. This asymmetry cannot simply be explained by texture in the absorber. Samples of guanidinium nitroprusside carefully prepared without pressing always yield an asymmetric quadrupole doublet, while samples of nitroprussides with inorganic cations prepared the same way show symmetric quadrupole doublets. When comparing these results it is tempting to speculate that the observed asymmetry in the quadrupole doublet of the powder sample of guanidinium nitroprusside is caused by the Goldanskii-Karyagin effect [2]. The absence of this effect in nitroprussides with inorganic cations is a strong evidence that both intra- and intermolecular vibrations are isotropic while in

guanidinium nitroprusside the vibrations in the crystal lattice are strongly anisotropic which results in the pronounced Goldanskii-Karyagin effect.

In 1977 Hauser and coworkers [3] discovered the existence of long-lived metastable states in sodium nitroprusside by Mössbauer investigations. Since then numerous nitrosyl complexes were the subject of intensive studies by means of many other methods [1,4–7]. Two long living metastable molecular conformations (MS_1 and MS_2) can be generated by irradiation with light in the spectral range 350–580 nm at temperatures below 200 K (MS_1) and 150 K (MS_2). The existence of these states has been evidenced by Mössbauer spectroscopy also in other nitroprussides [1,8]. While such states are of great interest for optical information storage with extremely high capacity at the same time the phenomenon itself is of great interest for fundamental research. Carducci *et al.* [9] offered an explanation of the nature of the observed metastable states MS_1 and MS_2 . In the MS_1 state the $(\text{NO})^+$ -group is inverted and in the new so-called isonitrosyl structure the bondings are $\text{N} - \text{C} - \text{Fe} - \text{O} - \text{N}$ instead of $\text{N} - \text{C} - \text{Fe} - \text{N} - \text{O}$ in the ground state (GS). For the case of the MS_2 state

^a e-mail: trautwein@physik.mu-luebeck.de

a side-on molecular conformation of bondings, $\text{N} - \text{C} - \text{Fe} \begin{matrix} \text{N} \\ \langle \\ \text{O} \end{matrix}$ has been proposed. The proposition

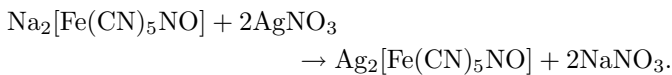
provided by Carducci *et al.* [9] is, however, in contradiction to the results obtained from neutron diffraction studies of deuterated sodium-nitroprusside single crystals in MS_1 state [10], because in this study the $(\text{NO})^+$ -group is reported not to be inverted.

In this contribution we present an investigation of the lattice vibrational anisotropy by Mössbauer measurements on powder samples of barium and guanidinium nitroprusside as well as on single-crystalline guanidinium nitroprusside. Guanidinium nitroprusside is especially suitable for angular-resolved measurements since all nitroprusside anions have almost the same orientation within the single crystal [11]. These structural features and the absence of crystal water determine this nitroprusside as especially promising for investigations of long-lived optically excited metastable states. In our work these states were populated using a simple illumination device.

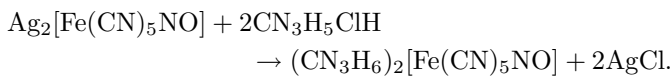
2 Material and methods

2.1 Guanidinium nitroprusside

$(\text{CN}_3\text{H}_6)_2[\text{Fe}(\text{CN})_5\text{NO}]$ is one out of numerous nitroprusside iron complexes, the best studied of which is the sodium nitroprusside $\text{Na}_2[\text{Fe}(\text{CN})_5\text{NO}]2\text{H}_2\text{O}$ often used as a velocity calibration standard for Mössbauer spectroscopy. The raw material for growing guanidinium nitroprusside single crystals has been synthesized from silver nitroprusside, which was produced from aqueous solution of sodium nitroprusside by adding AgNO_3 :



Treatment of the washed precipitate $\text{Ag}_2[\text{Fe}(\text{CN})_5\text{NO}]$ with guanidinium hydrochloride $\text{CN}_3\text{H}_5\text{ClH}$ in water yielded an aqueous solution of $(\text{CN}_3\text{H}_6)_2[\text{Fe}(\text{CN})_5\text{NO}]$:



The barium nitroprusside was synthesized following the known procedure of cation exchange reaction between $\text{Ag}_2[\text{Fe}(\text{CN})_5\text{NO}]$ and $\text{BaCl}_22\text{H}_2\text{O}$.

Single crystals of $(\text{CN}_3\text{H}_6)_2[\text{Fe}(\text{CN})_5\text{NO}]$ with a size of $10 \times 10 \times 50 \text{ mm}^3$ could be grown from the aqueous solution by slow evaporation of the solvent at about 310 K. (Space group: $Pnma$; lattice constants: $a = 8.943(1) \text{ \AA}$, $b = 10.240(2) \text{ \AA}$, $c = 16.143(2) \text{ \AA}$ with four nitroprusside anions per unit cell; density: $D = 1.511 \text{ g/cm}^3$). The conditions of the crystal growth, as well as chemical and structural properties of guanidinium nitroprusside are discussed in detail elsewhere [11,12]. For Mössbauer absorption measurements single crystals of about 1 mm thickness

have been used. The samples were cut from larger crystals of high quality with the surface normal being parallel to the crystallographic **a**-, **b**-, and **c**-direction (**a**-, **b**- and **c**-cut, respectively). Though it is relatively easy to obtain single crystals of barium nitroprusside, they were not grown for Mössbauer purposes because of the absence of Goldanskii-Karyagin effect, and because the very high absorption coefficient of the 14.4 keV Mössbauer radiation prohibits the application of this nitroprusside to further investigations. Our calculations of the absorption coefficient for 14.4 keV γ -quanta based on data from [13] show that barium nitroprusside has a much greater coefficient of absorption ($\mu_e = 32.94 \text{ cm}^2/\text{g}$) than guanidinium nitroprusside ($\mu_e = 11.99 \text{ cm}^2/\text{g}$).

2.2 Mössbauer absorption spectroscopy

Mössbauer spectra were recorded with a spectrometer in constant-acceleration mode with a $^{57}\text{Co}[\text{Rh}]$ source ($\sim 1.1 \text{ GBq}$). The velocity calibration was performed with a $\text{Na}_2[\text{Fe}(\text{CN})_5\text{NO}]2\text{H}_2\text{O}$ single crystal for which the quadrupole splitting (ΔE_Q) and the isomer shift (δ) are known with high accuracy [14,15]. The measured isomer shifts are referred to an α -Fe standard at room temperature. The experimental spectra were fitted by a sum of Lorentzian lines by means of a least-squares procedure. Measurements on oriented single crystals of guanidinium nitroprusside at room temperature were performed by mounting the single crystals on a goniometer which was placed between source and detector of the Mössbauer spectrometer.

The probability of recoilless absorption (Lamb-Mössbauer factor, f_{LM}), may be calculated from the area of the Mössbauer absorption lines. The experimental area $A(t)$ depends on the effective thickness t as [13]

$$A(t) = \frac{1}{2} N_\infty R \pi t \Gamma_A \exp(-t/2) [I_0(t/2) + I_1(t/2)]$$

$$t = n \sigma_0 f_{\text{LM}} \Gamma_N / \Gamma_A \quad (1)$$

where N_∞ is the number of counts at infinite velocity of the source (the absorber being fixed), R is the recoilless part of the γ -quanta in the window of the differential discriminator, Γ_N is the natural line width for ^{57}Fe (0.097 mm/s), Γ_A is the line width of the absorber, I_0 and I_1 are modified Bessel functions of the first kind and zeroth and first order, respectively, n is the number of ^{57}Fe nuclei per cm^2 (the natural abundance of the ^{57}Fe isotope is 2.19%), and $\sigma_0 = 2.57 \times 10^{-18} \text{ cm}^2$ is the maximum resonant absorption cross section.

In general, the absorption cross section σ of a particular line in a hyperfine spectrum of a single-crystalline absorber is given by a 2×2 matrix [14,16]

$$\sigma = \begin{vmatrix} \sigma_{11} & \sigma_{12} \\ \sigma_{21} & \sigma_{22} \end{vmatrix}, \quad (2)$$

where σ_{11} and σ_{22} represent the absorption of the two basic polarization directions, and σ_{12} and σ_{21}

the cross section of birefringence effects (Faraday effect, double refraction etc.). These cross sections are zero only for specific highly-symmetric directions in the crystal, otherwise analytical expressions of the cross sections have to be taken into account [14]. For example, at measurements in the mirror plane **ac** (the wave vector of the γ -quantum \mathbf{k}_γ lies in this plane) where there are two nonequivalent groups 1 and 2 of nitroprusside ions the analytical expressions for the cross sections are:

$$\left\{ \begin{array}{l} \sigma_{11}^1 = \frac{1}{2}\sigma_0 f_{LM}^1 \left[\frac{1}{2} \pm \frac{1}{4} \sqrt{\frac{3}{3+\eta^2}} (1-\eta) \right] \\ \sigma_{12}^1 = \sigma_{21}^1 = 0 \\ \sigma_{11}^2 = \frac{1}{2}\sigma_0 f_{LM}^2 \left[\frac{1}{2} \pm \frac{1}{4} \sqrt{\frac{3}{3+\eta^2}} (1-\eta) \right] \\ \sigma_{12}^2 = \sigma_{21}^2 = 0 \\ \sigma_{22}^1 = \frac{1}{2}\sigma_0 f_{LM}^1 \left[\frac{1}{2} \pm \frac{1}{4} \sqrt{\frac{3}{3+\eta^2}} \right. \\ \quad \left. \times (1 - 3 \sin^2(\Omega - \theta) + \eta \cos^2(\Omega - \theta)) \right] \\ \sigma_{22}^2 = \frac{1}{2}\sigma_0 f_{LM}^2 \left[\frac{1}{2} \pm \frac{1}{4} \sqrt{\frac{3}{3+\eta^2}} \right. \\ \quad \left. \times (1 - 3 \sin^2(\Omega + \theta) + \eta \cos^2(\Omega + \theta)) \right]. \end{array} \right. \quad (3)$$

f_{LM}^1 and f_{LM}^2 are the Lamb-Mössbauer factors of the two nonequivalent groups of nitroprusside ions in the **ac** plane which have slightly different orientations to the **c**-axis ($\pm 8^\circ$) according to [11,12]; η is the asymmetry parameter of the electric field gradient; θ is the angle between the main component of the electric field gradient tensor and the **c**-axis and Ω the angle between the wave vector of the γ -quantum \mathbf{k}_γ and the **c**-axis. The upper index of σ is for the two groups of nitroprusside ions, the upper sign in \pm is for $3/2 \rightarrow 1/2$, and the lower sign for $1/2 \rightarrow 1/2$ transitions. For this highly symmetric plane the σ_{12} and σ_{21} cross sections are zero. One can find more details and an extensive discussion on this case in [14]. From measurements with the γ -beam directing along the crystallographic **a**-, **b**- and **c**-axes and from additional angular-dependent measurements rotating the single crystal around a crystallographic axis perpendicular to the γ -beam direction, the values for $f_{LM}^{(a)}$, $f_{LM}^{(b)}$ and $f_{LM}^{(c)}$ and other parameters such as the electric field gradient (EFG) tensor and the mean-square displacement (MSD) tensor have been derived by a multiparameter fit.

2.3 Population conditions

MS₁ and MS₂ states have been populated in **a**- and **c**-cut single-crystal samples of guanidinium nitroprusside. The efficiency of the generation of excited states depends on the angle between the N – C – Fe – N – O axis of the nitroprusside anions and the electric field vector of the incident light. This angle should be close to 90° [8] which

implies that only suitable crystal cuts can be studied and the illumination must be preferably by polarized light. Laser light in the blue spectral range (frequently chosen 457.8 nm) populates about 50% of the sodium nitroprusside molecules in MS₁. In other single crystals the population was not so high: in Li₂[Fe(CN)₅NO]4H₂O 25% and in K₂[Fe(CN)₅NO]2.5H₂O only 13% [1]. The important polarization condition to achieve high population was fulfilled in all experiments. For population experiments with guanidinium nitroprusside a very simple and cheap self-made irradiation cell of twelve light-emitting diodes (LED product of Marl) was used. The diodes emit unpolarized light in the blue spectral region 450 ± 35 nm with an intensity of about 200 mcd each. The twelve diodes were connected in parallel, six diodes on each side of the crystal, using a 140 mA current source. A very precise determination of the light intensity was not achievable because the irradiation cell worked under conditions of a continuous-flow helium cryostat at 78 K. If suitable molecular orientations are met this irradiation system can successfully substitute the expensive and heavy Ar⁺-laser equipment that is commonly used.

3 Results and discussion

3.1 Mössbauer absorption studies on powder samples of barium and guanidinium nitroprussides and comparison of the vibrational anisotropy with X-ray structural analysis

Figure 1 shows Mössbauer spectra of barium and guanidinium nitroprusside taken from powder samples at room temperature. We chose this couple of nitroprussides because it has also been studied by X-ray structural analysis [11]. Thus, our Mössbauer spectroscopic investigations on the vibrational anisotropy of barium and guanidinium nitroprusside can be compared with the X-ray results. The values of the Lamb-Mössbauer factors f_{LM} are related to the thermal parameters $U_{ii}(\text{Fe})$ yielded by the refinement procedure of X-ray diffraction investigations. The vibrational anisotropy follows from the relation $f_{LM}^{ii} = \exp(-\mathbf{k}_\gamma^2 \langle x_{ii}^2 \rangle)$ assuming for the mean-square displacement parameters $\langle x_{ii}^2 \rangle \equiv U_{ii}(\text{Fe})$. Here \mathbf{k}_γ is the γ -quantum wave vector. Table 1 summarizes the available data about the Lamb-Mössbauer factors f_{LM} extracted either from U_{ii} or derived by Mössbauer spectroscopy.

The results from the powder sample in [1] as well as the results given in Figure 1 show that barium nitroprusside has a comparatively high Lamb-Mössbauer factor $f_{LM} = 0.30$ and does not show anisotropy (Goldanskii-Karyagin effect). Usually, the f_{LM} -factors of nitroprussides with an organic cation are two times smaller, *i.e.* for guanidinium nitroprusside we obtain the mean value $f_{LM} = 0.16$ and a well pronounced asymmetry in the crystal. In both crystals the individual f_{LM}^{ii} , as determined from U_{ii} , are different which makes one expect that both crystals should exhibit strong Goldanskii-Karyagin effect. The results in Figure 1 disproves this expectation. Only guanidinium nitroprusside exhibits this effect.

Table 1. Thermal parameters U_{ii} for barium and guanidinium nitroprusside [10], Lamb-Mössbauer factors f_{LM} extracted from U_{ii} and Lamb-Mössbauer factors measured with powder samples and single crystals by Mössbauer absorption spectroscopy [1] (and this work), and line intensity ratio I_+/I_- for powder samples.

Parameter		U_{11} in \AA^2	U_{22} in \AA^2	U_{33} in \AA^2	Orientation of V_{zz}
Compound	f_{LM}	$f_{LM}^{(a)}$ from U_{11}	$f_{LM}^{(b)}$ from U_{22}	$f_{LM}^{(c)}$ from U_{33}	I_+/I_- from U_{ii}
		$f_{LM}^{(a)}$ from Mö	$f_{LM}^{(b)}$ from Mö	$f_{LM}^{(c)}$ from Mö	I_+/I_- from Mö
Barium nitroprusside	powder sample	162×10^4	251×10^4	145×10^4	$V_{zz} \parallel \mathbf{b}$
	0.30(2)	0.421	0.262	0.461	0.94
	zero Goldanskii-Karyagin effect	—	—	—	0.99(2)
Guanidinium nitroprusside	powder sample	361×10^4	293×10^4	275×10^4	$V_{zz} \parallel \mathbf{c}$
	0.16(2)	0.145	0.209	0.230	1.06
	strong Goldanskii-Karyagin effect	0.118	0.174	0.202	1.08(2)

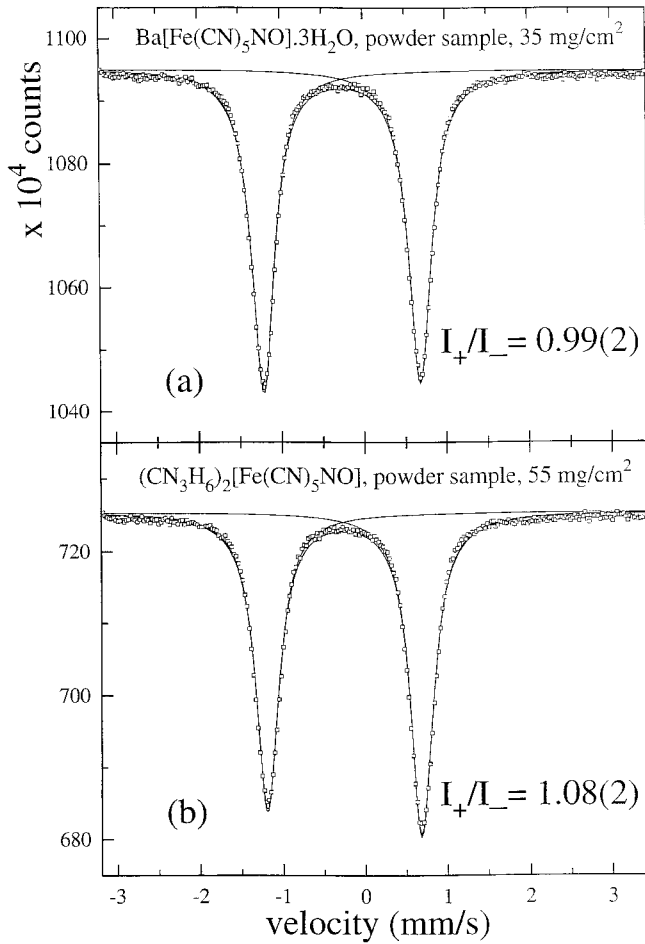


Fig. 1. Mössbauer spectra of (a) barium nitroprusside and (b) guanidinium nitroprusside recorded from powder samples at room temperature. The measured relative intensity ratio I_+/I_- as indicated.

In the following we use the f_{LM}^{ii} values as derived from U_{ii} to calculate Mössbauer line intensity ratios. The main component V_{zz} of the electric field gradient in barium nitroprusside is parallel to the \mathbf{b} -axis and the crystal

has the smallest f_{LM}^{ii} -factor along this crystal direction (Tab. 1). In guanidinium nitroprusside V_{zz} is parallel to the \mathbf{c} -axis, but in this direction the f_{LM}^{ii} -factor has its maximum. The relative intensity ratio I_+/I_- of the right hand ($3/2 \rightarrow 1/2, I_+$) and of the left hand ($1/2 \rightarrow 1/2, I_-$) line of the quadrupole doublets for crystals with anisotropic Lamb-Mössbauer factors can be received by integrating over the total solid angle taking into account that f_{LM} -factors are different for the different crystal directions. We calculated the expected anisotropy of the quadrupole doublets of barium and guanidinium nitroprussides following the theory of the Goldanskii-Karyagin effect [2] and using values for f_{\parallel} along V_{zz} and for f_{\perp} perpendicular to V_{zz} as derived from U_{ii} (Tab. 1). According to this procedure the doublets of both nitroprussides have to be asymmetric: in the case of barium nitroprusside $I_+/I_- = 0.94$ (the right hand line has lower intensity) and for guanidinium nitroprusside $I_+/I_- = 1.06$ (the left hand line has lower intensity). The line intensity ratio in guanidinium nitroprusside, measured by Mössbauer spectroscopy (Fig. 1b) $I_+/I_- = 1.08(2)$ is in good agreement with the predicted value of 1.06. However, the quadrupole doublet of barium nitroprusside (Fig. 1a) is practically symmetric, $I_+/I_- = 0.99(2)$, and therefore this crystal possesses negligible vibrational anisotropy. This pretended contradiction between X-ray and Mössbauer results has been reported earlier. Grant *et al.* [14] have compared the mean-square displacement parameters $\langle x^2 \rangle$ of the iron sites in sodium nitroprusside measured by Mössbauer spectroscopy with the corresponding thermal parameters U_{ii} extracted from an X-ray structure determination by Monoharan *et al.* [17]. The two methods have yielded considerably different results. Parak *et al.* [18] have observed similar discrepancies in myoglobin. They have provided an explanation which also holds for the present case: for X-ray diffraction the typical time of interaction (Rayleigh scattering) is of the order 10^{-13} s, for Mössbauer spectroscopy this time range is larger, *i.e.* $10^{-7} \div 10^{-8}$ s. Evidently, the two methods yield information about vibrational anisotropy and dynamical processes in two totally different regions of the time scale. In the short time scale ($\sim 10^{-13}$ s) the vibrational

Table 2. Mössbauer parameters of guanidinium nitroprusside single crystals for different axis orientations, recorded at room temperature: isomer shift δ , quadrupole splitting ΔE_Q , and left and right line widths Γ_- and Γ_+ , respectively, in mm/s, and line intensity ratio I_-/I_+ .

Parameter	δ^a	ΔE_Q	Γ_-	Γ_+	I_-/I_+
Sample	[mm/s]	[mm/s]	[mm/s]	[mm/s]	
a-cut	-0.252(3)	1.852(3)	0.248(3)	0.244(3)	1.62(1)
b-cut	-0.249(3)	1.850(3)	0.256(3)	0.257(3)	1.62(1)
c-cut	-0.252(3)	1.854(3)	0.233(3)	0.266(3)	0.44(1)

^a relative to α -Fe at room temperature.

properties of the iron atoms in the nitroprusside cations are detected and found to be anisotropic in both crystals, as it is shown by the X-ray analysis. In the long time scale ($10^{-7} \div 10^{-8}$ s) the long-wavelength, low-energy lattice phonons, causing a low Lamb-Mössbauer factor, reflect the vibrational anisotropy of the crystal as a whole. Thus the considerably smaller Lamb-Mössbauer factor of guanidinium nitroprusside provides evidence that only in this case (and not in barium nitroprusside) anisotropic lattice vibrations are detected and cause a measurable Goldanskii-Karyagin effect. At the low-frequency limit the Debye approximation should hold. When using the equation for the Debye temperature [2], $\theta_D = \sqrt{\frac{-6E_R T}{k \ln(f_{LM})}}$, $T \geq \theta_D/2$, where E_R is the recoil energy of the iron nucleus, k the Boltzmann constant, T the absolute temperature and $f_{LM} \sim 0.1$ the mean value of the Lamb-Mössbauer factor for guanidinium nitroprusside, the Debye temperature takes the value $\theta_D \sim 130$ K. The corresponding shortest phonon wavelength $\lambda \sim 7$ Å is derived from $\lambda = hc/k\theta_D$, with h being the Planck constant and using for the velocity of sound the value $c = 2000$ ms⁻¹. A corresponding calculation for barium nitroprusside with $f_{LM} \sim 0.3$ yields a slightly shorter phonon wavelength (~ 5 Å). Thus, the low-frequency vibrations, with wavelengths $\gtrsim 7$ Å (and also $\gtrsim 5$ Å) are susceptible to structural anisotropies which affect the vibrational mean-square displacement of the nitroprusside anions as a whole.

3.2 Mössbauer absorption studies on single-crystalline guanidinium nitroprusside

Figure 2 shows Mössbauer spectra of guanidinium nitroprusside single crystals recorded at room temperature with the **a**, **b**, and **c** crystallographic axes parallel to the incident radiation. The Mössbauer parameters δ and ΔE_Q obtained for guanidinium nitroprusside (Tab. 2) are very close to the parameters of a large number of iron nitroprussides already published [1]. The measured line-intensity ratio I_-/I_+ of the **a**- and **b**-cut crystals are practically identical, whereas for the **c**-cut crystal a significantly different intensity ratio of the two quadrupole lines is observed (Tab. 2 and Fig. 2). In case of threefold or higher molecular symmetry, which applies for guanidinium nitroprusside [11], the asymmetry parameter of the EFG is

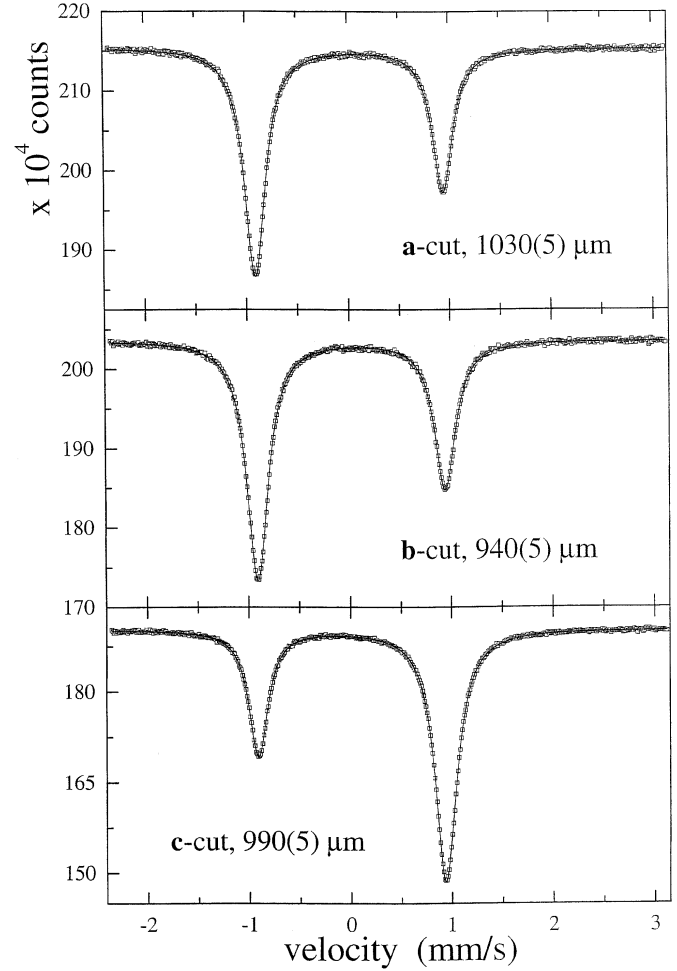


Fig. 2. Mössbauer spectra of guanidinium nitroprusside single crystals recorded at room temperature with the **a**, **b**, and **c** crystallographic axes parallel to the incident radiation and with thicknesses as indicated. Least-squares fits (solid lines) using Lorentzians yield hyperfine parameters as summarized in Table 2.

zero ($\eta = 0$) and hence the intensity ratio of the right hand ($3/2 \rightarrow 1/2, I_+$) and the left hand ($1/2 \rightarrow 1/2, I_-$) line of the quadrupole doublets is (in the thin absorber approximation and for positive EFG component V_{zz}) given by [14]

$$\frac{I_-}{I_+} = \frac{2/3 + \sin^2 \beta}{1 + \cos^2 \beta}, \quad (4)$$

with β describing the angle between the γ -beam propagation and the symmetry axis of the EFG tensor. For $\beta = 90^\circ$ the intensity ratio is 5:3, which is close to the observed ratios for the **a**- and **b**-cut crystals (~ 1.6) whereas for $\beta = 0^\circ$ the ratio is 1:3, from which the observed value for the **c**-cut crystal (0.44) slightly deviates. From these results it is evident that in guanidinium nitroprusside the symmetry axis of the EFG tensor of the $[\text{Fe}(\text{CN})_5\text{NO}]^{2-}$ anions is close to but not completely coincident with the crystallographic **c**-axis. This is consistent with the X-ray structure determination of the guanidinium

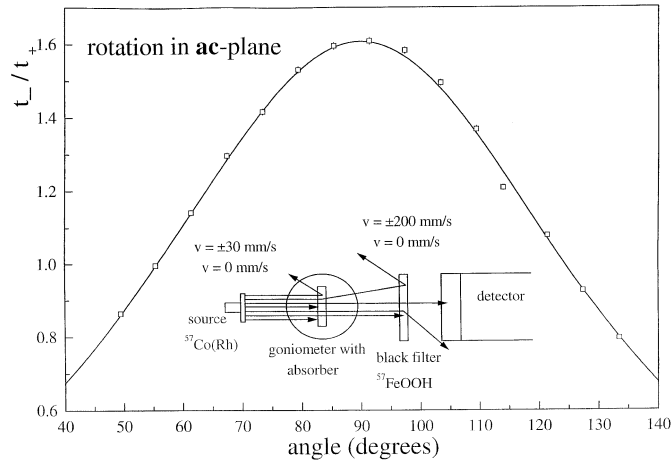


Fig. 3. Angular-dependent ratio t_-/t_+ of the effective thicknesses of the left and right lines, t_- and t_+ , of the quadrupole doublet of guanidinium nitroprusside as obtained from a measurement (open squares) rotating the single crystal by Ω (see Eq. (3)) around the crystallographic **b**-axis (which in this case is perpendicular to the γ -beam) and keeping the γ -beam within the **ac**-plane. The angle of 90° corresponds to the situation of **c**-axis perpendicular to γ -beam. The inset shows the experimental setup. The solid line results from a multiparameter fit of the experimental data.

nitroprusside crystal [11,12] which yields two different orientations of the intramolecular symmetry axis ($N-C-Fe-N-O$) of the $[\text{Fe}(\text{CN})_5\text{NO}]^{2-}$ anions which deviate by about $\pm 8^\circ$ from the crystallographic **c**-axis. Consequently, all $[\text{Fe}(\text{CN})_5\text{NO}]^{2-}$ anions in the crystal have nearly the same orientation, which is an excellent prerequisite to study the vibrational anisotropy in the equatorial and axial direction.

Figure 3 exhibits the angular-dependent ratio t_-/t_+ of the effective thicknesses of the left and right hand lines, t_- and t_+ of the quadrupole doublet of guanidinium nitroprusside as obtained from rotating the single crystal by Ω around the crystallographic **b**-axis which in this case is perpendicular to \mathbf{k}_γ . The solid line in Figure 3 results from calculating t_-/t_+ according to equation (1) taking into account polarization effects and the precise cross section equations for σ_{21} and σ_{22} , equation (3). In order to increase the accuracy of the fit parameters $f_{\text{LM}}^{(a)}$, $f_{\text{LM}}^{(b)}$ and $f_{\text{LM}}^{(c)}$, this procedure requires as many as possible different crystal orientations. The necessary angular-dependent changes of geometrical thickness, which the γ -beam has to transmit, were carefully included. The fit procedure also requires the careful determination of the recoilless part R of the γ -quanta in the window of the differential discriminator.

We have applied the “control absorber” method with “black filter” (Fig. 3, inset) to determine R . Moving the “black filter” ($^{57}\text{FeOOH}$), which was placed in front of the detector, at very high velocity (± 200 mm/s) excludes resonance absorption in the “black filter” (only nonresonant absorption in the “black filter” decreases the beam inten-

sity by about 10%). Under these conditions Mössbauer absorption spectra, such as those presented in Figure 2, were accumulated. With both source (± 30 mm/s) and the “black filter” (± 200 mm/s) moving at high velocity resonance absorption in the guanidinium nitroprusside single crystal and in the “black filter” is excluded. In this case the detector registers both the transmitted resonant and nonresonant radiation of the source (N_1). For both source and “black filter” being fixed (0 mm/s) the detector counts only the nonresonant radiation (N_2) because the resonant component is absorbed in the “black filter”. Hence, R is obtained from the expression

$$R = \frac{N_1 - N_2}{\varepsilon N_1}, \quad (5)$$

with ε being the “black filter” resonance absorption ability [19]. This correction must be taken into account since the “black filter” (15.4 mg/cm^2 $^{57}\text{FeOOH}$ with an effective thickness of about 100) cannot absorb all resonant γ -quanta. The measured counts N_2 are the sum of nonresonant radiation and a very small fraction of resonant γ -quanta which pass through the “black filter”. Given the value of the “black filter” effective thickness, we can calculate the resonance absorption ability or the so-called “blackness” of the filter using equation (1). Calculations show that the measured values of R are about 5% lower than the theoretical ones. For the “black filter” used here the values of R should be corrected with $\varepsilon = 0.95$.

In addition to the measurements shown in Figure 3 angular-dependent measurements have been performed keeping \mathbf{k}_γ within the **ab**- and the **bc**-plane, respectively (not shown). The combined experimental data obtained from the various single-crystal orientations with respect to \mathbf{k}_γ provide the information for a successful multiparameter fit of Mössbauer parameters among which the significant anisotropy of f_{LM} is the most striking result: $f_{\text{LM}}^{(a)} = 0.118(8)$, $f_{\text{LM}}^{(b)} = 0.174(8)$, $f_{\text{LM}}^{(c)} = 0.202(8)$. The average of these values is consistent with the Lamb-Mössbauer factor $f_{\text{LM}} = 0.16$ that has been determined for a powder sample of guanidinium nitroprusside [1]. The large difference between $f_{\text{LM}}^{(a)}$ and $f_{\text{LM}}^{(c)}$ provides clear evidence for lattice vibrational anisotropy.

Although all $[\text{Fe}(\text{CN})_5\text{NO}]^{2-}$ anions have almost same orientation their stereostructural surroundings in the three principal crystal directions are quite different, *e.g.*, the normals of the two planar guanidinium cations, which are not related to one another by a symmetry transformation, lie in the **ac**-plane having angles 35° and 55° with the **c**-axis, respectively [12]. In addition the chemical bonding between the large organic guanidinium cations and the nitroprusside anions is very weak because of the large distance of 3.12 \AA between the H-atoms in $(\text{CN}_3\text{H}_6)^+$ and the N-atoms in $[\text{Fe}(\text{CN})_5\text{NO}]^{2-}$ [12], in contrast to the situation of nitroprusside with inorganic counterions where the distance between cations and anions is much smaller. Hence, it is the large and anisotropic vibrational mean-square displacement $\langle x^2 \rangle$ of $[\text{Fe}(\text{CN})_5\text{NO}]^{2-}$ as a whole which causes the relatively small but strongly

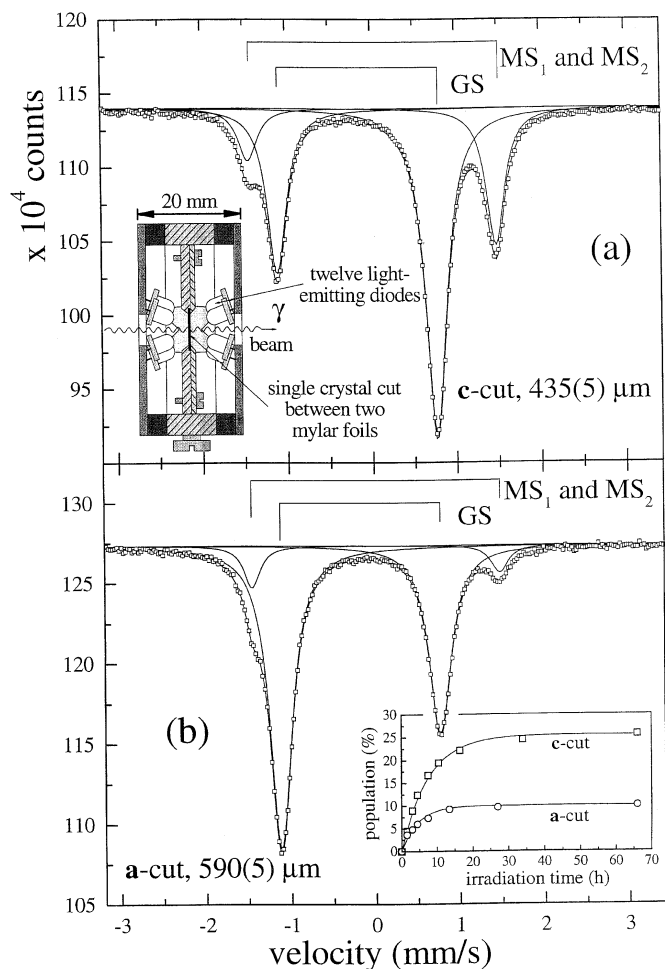


Fig. 4. Mössbauer spectra of guanidinium nitroprusside single crystals with ground state (GS) and light-excited metastable states MS_1 and MS_2 at 77 K. (a) Crystallographic *c*-axis parallel to the incident radiation; inset shows the illumination cell. (b) Crystallographic *a*-axis parallel to the incident radiation; inset shows population saturation observed for *c*- and *a*-cuts.

anisotropic Lamb-Mössbauer factor in guanidinium nitroprusside. Since the Lamb-Mössbauer factor is the product of an *intra*-molecular contribution f_{LM}^{mol} and an *inter*-molecular (lattice) contribution f_{LM}^{lat} it is clear that the observed asymmetry of line intensities in powder samples of guanidinium nitroprusside (Fig. 1b) is solely due to the anisotropy of f_{LM}^{lat} , while f_{LM}^{mol} is isotropic as in the nitroprussides with inorganic cations. Therefore the initial guess, that this asymmetry of line intensities of powder samples cannot be explained by texture in the absorber but is caused by the Goldanskii-Karyagin effect, is confirmed by these measurements on single crystals.

3.3 Population of the metastable excited states

The structural features of guanidinium nitroprusside make it possible to achieve maximum population of the excited states even when irradiating the crystal with unpolarized light. In a *c*-cut crystal all molecular axes

$C-N-Fe-N-O$ of the nitroprusside anions are orientated almost perpendicular to the crystal surface. Thus when illuminating the crystal at an angle of nearly 90° to its surface the light electric field vector will always be perpendicular to the molecular symmetry axes despite of the fact that the illuminating light is not polarized. In this case the crystal can be populated close to the maximum attainable saturation. The Mössbauer beam propagates through an opening of the diode circuits and is also oriented normal to the crystal surface (Fig. 4a, inset).

In accordance with our estimate, the *c*-cut allows to achieve considerable population of excited states (Fig. 4a). Assuming equal values of the Lamb-Mössbauer factors for all states the following populations are derived: $I_{GS} \cong 74\%$, $I_{MS_1+MS_2} \cong 26\%$. The Mössbauer parameters of the excited metastable states MS_1 and MS_2 , $\delta = -0.010(3)$ mm/s and $\Delta E_Q = 2.929(3)$ mm/s, are in accordance with data published for other nitroprussides [1,3,5,8]. Heating the target up to 150 K (temperature higher than that at which MS_2 decays [20]) and after one hour cooling to 77 K resulted in a change of the spectrum. About 7% of MS_1 and MS_2 is transferred back to the ground state.

For the other crystal orientation (*a*-cut) the molecular symmetry axes are perpendicular to the direction of the illuminating light. In this case the percentage of molecules in metastable states MS_1 and MS_2 is only 10.5% (Fig. 4b). In the inset of Figure 4b the saturation behaviour of the population, observed in *a*- and *c*-crystal directions is shown. Hauser *et al.* have obtained saturation populations of $\sim 50\%$ for single crystals and about 1/3 of that for frozen solution of sodium nitroprusside, using laser light [8]. Keeping in mind that the molecular symmetry axis is not completely parallel to the *c*-axis in guanidinium nitroprusside and that the LEDs do not irradiate exactly along the normal of the crystal surface the ratio of populations obtained for “polarized” (*c*-cut) and “unpolarized” (*a*-cut) conditions (Fig. 4b, inset) is close to the value 1/3 observed for sodium nitroprusside using laser light (*vide supra*). The energy density needed to achieve saturation of excited states (~ 2500 Ws/cm²) is in both experiments, using laser or LED irradiation about the same. In summary, we note that a simple LED cell can successfully substitute the Ar⁺-laser equipment that is so far used for populating excited states in nitroprussides.

4 Conclusion

Guanidinium nitroprusside exhibits a pronounced anisotropy of the Lamb-Mössbauer factor f_{LM} as observed in single crystals with different orientations of their principal crystallographic axes with respect to the γ -beam. The anisotropy of f_{LM} is ascribed to the anisotropic vibrational mean-square displacement of the nitroprusside anions as a whole. This behaviour proves that the observed asymmetry of line intensities of powder samples is due to the Goldanskii-Karyagin effect. The small values of f_{LM} result from the very weak chemical bonding between

the guanidinium cations and the nitroprusside anions. The anisotropy of the thermal parameters U_{ii} for the iron atom in barium nitroprusside observed in X-ray structural studies does not manifest itself in Mössbauer spectroscopy: powder samples of barium nitroprusside do not exhibit the Goldanskii-Karyagin effect. This difference in observing crystal anisotropies is due to the different time scales of the two methods.

The recently discovered metastable states of the nitroprusside anions which can be optically excited were populated up to 26% in c-cut guanidinium nitroprusside. This makes guanidinium nitroprusside besides sodium nitroprusside a favorable candidate with respect to its population coefficient. Optical pumping in our experiments was carried out by means of a simple self-made illumination cell with twelve LEDs.

V. R. gratefully acknowledges the support by the Volkswagen-Foundation and by the Alexander von Humboldt-Foundation. We thank K.-H. Finder for the technical assistance with the population experiments.

References

1. V. Rusanov, V. Angelov, J. Angelova, Ts. Bonchev, Th. Woike, Hyung-sang Kim, S. Haussühl, J. Solid State Chem. **123**, 39 (1996).
2. V.I. Goldanskii, E.F. Makarov, *Chemical Applications of Mössbauer Spectroscopy* (Academic Press, New York, London, 1968), p. 102.
3. U. Hauser, V. Oestreich, H.D. Rohrweck, Z. Phys. A **280**, 125 (1977); **284**, 9 (1978).
4. Th. Woike, W. Krasser, P.S. Bechthold, S. Haussühl, Phys. Rev. Lett. **53**, 1767 (1984).
5. Th. Woike, W. Kirchner, Hyung-sang Kim, S. Haussühl, V. Rusanov, V. Angelov, S. Ormandjiev, Ts. Bonchev, A.N.F. Schroeder, Hyperfine Interact. **77**, 265 (1993).
6. J.A. Guida, O.E. Piro, P.J. Aymonino, J. Inorg. Chem. **34**, 4113 (1995).
7. Y. Morioka, S. Takeda, H. Tomizawa, E. Miki, Chem. Phys. Lett. **292**, 625 (1998).
8. U. Hauser, W. Klimm, L. Reder, T. Schmitz, M. Wessel, H. Zellmer, Phys. Lett. A **144**, 39 (1990).
9. M.D. Carducci, M.R. Pressprich, P. Coppens, J. Am. Chem. Soc. **119**, 2669 (1997).
10. M. Rüdlinger, J. Schefer, G. Chevrier, N. Furer, H.V. Guedel, S. Haussühl, G. Hegel, P. Schweiss, T. Vogel, T. Woike, H. Zöllner, Z. Phys. B **83**, 125 (1991).
11. C. Retzlaff, W. Krumbe, M. Dörrfel, S. Haussühl, Z. Kristallogr. **189**, 141 (1989).
12. C. Retzlaff, Thesis, Universität Köln, Mathematisch-Naturwissenschaftliche Fakultät, 1987.
13. Ts. Bonchev, St. Statev, H. Neykov, C. R. Acad. Bulg. Sci. **33**, 611 (1980).
14. R.W. Grant, R.M. Housley, U. Gonser, Phys. Rev. **178**, 523 (1969).
15. W.T. Oosterhuis, G. Lang, J. Chem. Phys. **50**, 4381 (1969).
16. U. Gonser, H. Fischer, in *Mössbauer Spectroscopy II*, edited by U. Gonser (Springer, Berlin, 1981), pp. 99-137.
17. P.T. Monoharan, W.C. Hamilton, Inorg. Chem. **2**, 1043 (1963).
18. F. Parak, H. Hartmann, K.D. Aumann, H. Reuscher, G. Rennekamp, H. Bartunik, W. Steigemann, Eur. Biophys. J. **15**, 237 (1987).
19. V. Angelov, V. Rusanov, Ts. Bonchev, Th. Woike, S. Haussühl, Z. Phys. B **83**, 39 (1991).
20. H. Zöllner, W. Krasser, Th. Woike, S. Haussühl, Chem. Phys. Lett. **161**, 497 (1989).